CONF-8811181-1

The Kicked Rydberg Atom: Regular and Stochastic Motion

Joachim Burgdörfer

Department of Physics, University of Tennessee, Knoxville, TN 37996-1200

and

Oak Ridge National Laboratory, Oak Ridge, TN 37831-6377

ABSTRACT

We have investigated the dynamics of a three-dimensional classical Rydberg atom driven by a sequence of pulses. Both the deterministic system with periodic pulses and the closely related "noisy" system with random pulses have been studied in parallel. The Lyapunov exponent is calculated as a function of pulse height and the angular momentum of the initial state. We find differences between noisy and deterministic perturbations to be most pronounced for small pulse heights. Low angular momentum orbits show enhanced diffusion in agreement with recent experimental data for ion-solid interaction.

1. INTRODUCTION

The dynamics of simple, non-separable Hamiltonian systems with two or more ($n \geq 2$) degrees of freedom has gained considerable interest, both experimentally and theoretically. In their pioneering work Henon and Heiles[1] have found that two harmonic oscillators coupled by a non-linear perturbation possess a divided phase space with intermingled regions of regular and chaotic motion. Subsequent discovery of similar properties in a wide variety of systems ranging from the kicked rotor[2] to the hydrogen atom in a microwave field[3] have provided clear evidence for the universality of irregular dynamics[4] in Hamiltonian systems.

Topologically, regular motion is confined to n dimensional submanifolds ("KAM tori[5]) of the $2n$ dimensional phase space while chaotic motion explores regions of the $(2n - 1)$ dimensional energy hypersurface. The occurrence of chaotic motion is therefore possible for $n \geq 2$. For later reference we note that time-dependent Hamiltonian systems with

$n - 1$ degrees of freedom are topologically equivalent to time-independent systems with n degrees of freedom.

On a more intuitive level, chaotic motion is characterized by an extreme sensitivity to initial conditions. Nearby initial conditions separate exponentially leading to an exponential growth of small uncertainties and rendering the evolution to be unpredictable despite the deterministic nature of the motion. In general, the fraction of the phase space filled by chaotic orbits grows with increasing strength of a non-separable perturbation. In the limit of very strong perturbations almost all KAM tori disappear, allowing for a full exploration of the energy hypersurface. The system is then a K system[5], and in particular, "mixing". The latter property is of fundamental importance for many different fields such as statistical mechanics, plasma physics, and astronomy.

Small atomic systems provide an ideal testing ground for basic concepts of Hamiltonian non-linear dynamics. With the aid of collisional and laser excitation to provide state-selective preparation of atoms, it has become possible to accurately "tune" the relative strength of the non-integrable perturbation (for example, by an external field) relative to the intra-atomic Coulomb field. Theoretically, the structure of light atoms can be calculated with a high degree of accuracy. The calculation of the chaotic dynamics is therefore unaffected by uncertainties in the static structure or in the underlying forces. Prime examples for the study of chaotic dynamics in atoms, both classically and quantum mechanically, are the hydrogen atom in a strong static magnetic field[6], and the microwave ionization of hydrogen[3].

In the following, we present a progress report on our study of the classical Rydberg atom in the presence of δ-shaped pulses of an electric field with a time-dependent Hamiltonian

$$H(t) = \frac{p^2}{2} - \frac{1}{r} - z \sum_i \Delta P_i \delta(t - t_i). \qquad (1)$$

The amplitude of the pulse ("kick") is denoted by ΔP_i and the time at which the pulse occurs is denoted by t_i. For the pulse heights ΔP_i and the time between adjacent pulses, $\Delta t_i = t_{i+1} - t_i$ we used two different models:

a) a stochastic sequence $(\Delta t_i, P_i)$. In this case the system is "noisy", i.e. indeterministic. The perturbation itself is stochastic. We will refer to this type of stochasticity as extrinsic stochasticity.

b) a strictly periodic sequence with

$$\Delta P_i = (-1)^i \Delta P$$

and

$$\Delta t_i = T/2, \tag{2}$$

where T is the period of the sequence of alternating pulses. In this case the perturbation is deterministic. The stochasticity observed in the deterministic system will be referenced in the following as intrinsic. The limit of periodic pulses has been previously investigated for the one-dimensional[7,8,9] and three-dimensional [10] model.

The motivation for the present study is threefold: firstly, the model of the "kicked" Rydberg atom provides an approximate description for the evolution of excited states around swift ions penetrating solids. The momentum transfer ΔP_i by the "kicks" results from two-body collisions between the Rydberg electron and the ionic cores or the conduction electrons of the solids. Scattering processes in a solid are in general strongly stochastic unless very special conditions like channeling are met. Even in this case scattering at conduction electrons lacks strict periodicity and low-level noise will persist. The approximation of δ-shaped pulses is justified if the orbital period $T = 2\pi \omega_a^{-1}$ is large compared to the collision time $t_c = d/v_p$ where d is the static screening length of the medium. Secondly, Eq. (1) provides in the case of periodic pulses a simple model for the microwave ionization problem. While in detail quite different[9] the kicked hydrogen atom shares many features

3

with the sinusoidally perturbed hydrogen atom. In particular, its classical dynamics possesses a region of intrinsic chaoticity. Thirdly, Eq. (1) is computationally simple enough to study the long-time evolution of a three-dimensional system which permits the possible occurrence of Arnold diffusion[11], i.e. the slow diffusion due to the "Arnold web" connecting all stochastic regions in phase space. Little is known about the speed and quantitative significance of Arnold diffusion in a realistic physical system.

In the following, we report on first results of the numerical study of (1). Our primary focus here is on the comparative study of extrinsic and intrinsic stochasticity, both simultaneously present in (1) and on the angular momentum (ℓ) dependence of the stochastic motion. The latter is of importance for the understanding of the ℓ "diffusion" observed in ion-solid collisions[12,13], Rydberg atom-gas collisions[14,15], the ℓ mixing in strong fields[3] and in plasmas. Atomic units are used unless otherwise stated.

2. METHOD

The equation of motion generated by the Hamiltonian (1)

$$\frac{d}{dt}\vec{v} = -\frac{\vec{r}}{r^3} + \hat{z}\sum_i \Delta P_i \delta(t - t_i) \tag{3}$$

can be cast into the form of a discrete mapping connecting the phase space coordinates between adjacent kicks. This follows from the fact that the perturbation is δ-shaped, i.e. the evolution between adjacent kicks proceeds on an unperturbed Coulomb orbit. Denoting the phase space coordinates just before the ith kick by $\vec{r}_i = \vec{r}_i(t = t_i - \epsilon), \vec{v}_i = \vec{v}(t = t_i - \epsilon)$ the non-linear mapping T,

$$\begin{pmatrix} \vec{r}_{i+1} \\ \vec{v}_{i+1} \end{pmatrix} = T \begin{pmatrix} \vec{r}_i \\ \vec{v}_i \end{pmatrix} \tag{4}$$

can be constructed through a sequence of mappings

$$T = T_{\Delta t} \circ T_{\Delta P} \tag{5}$$

where $T_{\Delta P}$ effects the change of momentum due to the kick.

$$\begin{pmatrix} \vec{r}(t_i + \epsilon) \\ \vec{v}(t_i + \epsilon) \end{pmatrix} = \begin{pmatrix} \vec{r}_i(t_i - \epsilon) \\ \vec{v}_i(t_i - \epsilon) + \Delta P_i \hat{z} \end{pmatrix} = T\Delta P \begin{pmatrix} \vec{r}_i(t_i - \epsilon) \\ \vec{v}_i(t_i - \epsilon) \end{pmatrix} \tag{6}$$

and $T_{\Delta t}$ denotes the evolution on the unperturbed Coulomb (Kepler) orbit[16] between $t_i + \epsilon$ and $t_{i+1} - \epsilon$. In the case of the periodic pulses, the two-fold application of (4) corresponds to the evolution of the phase space coordinates during one period. The mapping (6) allows for a simple intuitive interpretation: The electron describes a (not necessarily random) "walk" in Coulomb state space (Fig. 1). The walk will be random when the dynamics becomes stochastic. The equation of motion (3) possesses axial symmetry, i.e. the azimuthal angle ϕ is cyclic and the conjugate momentum, the angular momentum component L_z, is conserved. Upon a canonical transformation, Eq. (6) can be rewritten as a four-dimensional non-linear mapping

$$\begin{pmatrix} n_{i+1} \\ \tau_{i+1} \\ \ell_{i+1} \\ \psi_{i+1} \end{pmatrix} = T \begin{pmatrix} n_i \\ \tau_i \\ \ell_i \\ \psi_i \end{pmatrix}, \tag{7}$$

where n_i is the classical action corresponding to the principal quantum number, τ_i is the conjugate angle variable (the mean anomaly), ℓ_i is the total angular momentum and ψ_i is its conjugate angle variable. For simplicity we use for the mappings (6) and (7) the same symbol. For later reference we note that the mapping (7) involving action-angle variables is applicable only to finite motion (i.e., bound states).

The mapping (7) can be easily iterated for a large number of kicks ($\gtrsim 10^5$). The most time consuming part is the solution of the transcendental equation for the eccentric anomaly[16] of the Kepler orbit. In the limiting case of periodic pulses the Hamiltonian (Eq. 1) closely resembles the Hamiltonian for the microwave ionization problem. Fourier expansion of (1) leads to

$$H(t) = \frac{p^2}{2} - \frac{1}{r} - z\frac{4\Delta P}{T}\cos \omega t - z\frac{4\Delta P}{T}\sum_{s=1}^{\infty}\cos(2s + 1)\omega t. \tag{8}$$

5

The first three terms in (8) represent the Hamiltonian for the hydrogen in a microwave field where the $4\Delta P/T$ corresponds to the effective field amplitude. The presence of higher harmonics suggests that a large number of additional first-and higher order resonances will make the pulsed system[11] more unstable and more chaotic than the monochromatically perturbed system. The increase of stochasticity means that the threshold value of the field strength for global stochasticity is lower than for the microwave Hamiltonian. This hypothesis is in line with results for the 1D hydrogen with impulsive perturbation[9].

The quantitative analysis of (7) can be simplified due to scaling properties of the classical dynamics. Results for one given set of $(n, \ell, \omega, \Delta P)$ are generic for a family of orbits $(n', \ell', \omega', \Delta P)$ generated by a mechanical similarity transformation. For an initial state with energy $\epsilon = -1/2n^2$ all elements of the family generated by a continuous similarity transformation with $\beta > O$,

$$(\epsilon/\beta, \sqrt{\beta}\ell, \Delta P/\sqrt{\beta}, \omega/\beta^{3/2}) \tag{9}$$

are equivalent for identical phase and Euler angles. It is, therefore, sufficient to investigate the dynamics for one given value of n(or ϵ). The strength of the perturbation can be characterized by its scaled pulse height

$$\Delta \tilde{P} = \Delta P/p_a = n\Delta P, \tag{10}$$

where $p_a = 1/n$ is the characteristic momentum of the orbital motion and

$$\tilde{\omega} = \omega/\omega_a = n^3 \omega \tag{11}$$

is the scaled frequency of the kicks. The atomic frequency is denoted by $\omega_a = n^{-3}$. Finally, it is convenient to introduce a scaled angular momentum $\tilde{\ell} = \ell/n$ which varies between 0 and 1. For a noisy system the characteristic perturbation parameters refer to their respective ensemble averages $< \Delta \tilde{P} >$ and $< \tilde{\omega} >$.

The frequently invoked method of Poincare surface of sections for analyzing the dynamics in time-dependent systems with one degree of freedom[4] is not directly applicable to (7) since the stroboscopic snapshots taken after each time step lie on a four-dimensional manifold. Projecting out one coordinate results in a three-dimensional manifold rather than a plane (i.e., a "surface of section"). However, a qualitative insight can be gained from a simultaneous projection of this four-dimensional manifold onto two perpendicular planes. Fig.2 shows the projection onto the (n, τ) and (ℓ, ψ) planes for the initial conditions $n_0 = 100, \ell_0 = 67.4, \tau_0 = 1.233, \psi_0 = 4.349$ and a periodic perturbation with frequency $\tilde{\omega} = 3/2$. Note that the azimuthal angle of the $\vec{\ell}$ vector is cyclic while the polar angle $\theta = 0.4466$ is determined by the conserved value of $\ell_z = 60.79$. For a scaled amplitude $\Delta \tilde{P} = 2. \times 10^{-2}$ corresponding to $\Delta P = 2 \times 10^{-4}$ (Fig. 2a) the evolution over 1000 periods (k=2000) produces topologically simple structures which reflect the existence of KAM tori in the low-dimensional manifold. A slight increase of the amplitude to $\Delta \tilde{P} = 3.5 \times 10^{-2}$ (Fig. 2b) leads obviously to a break-down of the torus and to a chaotic motion.

A quantitative measure for the chaoticity can be found by an analysis of the eigenvalue spectrum of the linear tangential mapping defined through the Jacobian matrix A^k of the k-fold iterated mapping T^k,

$$A^k = \frac{\partial(n_k, \tau_k, \ell_k, \psi_k)}{\partial(n_o, \tau_o, \ell_o, \psi_o)}. \tag{12}$$

Since the Hamiltonian mapping is symplectic[5] the eigenvalue spectrum of A^k is reflexive, i.e. the spectrum consists either of a quadruple of eigenvalues

$$(\alpha, \alpha^*, 1/\alpha, 1/\alpha^*) \tag{13a}$$

if α is complex or of two pairs of eigenvalues

$$(\alpha_1, 1/\alpha_1, \alpha_2, 1/\alpha_2) \tag{13b}$$

if the eigenvalues are real.

The motion is stable if all eigenvalues lie on the complex unit circle and becomes unstable if at least one α leaves the unit circle ($|\alpha| > 1$). According to Krein's theorem[5] this occurs if two eigenvalues rotating on the unit circle in the opposite direction undergo an "avoided crossing" pushing one eigenvalue inside ($|\alpha| < 1$) and the other outside the unit circle ($|\alpha| > 1$). For the latter we can define a positive Lyapunov exponent of the k-fold iterated tangential mapping A^k,

$$\lambda^{(k)} = \frac{1}{k} \ell n |\alpha^{(k)}| \tag{14}$$

In the special case k=1, we call $\lambda^{(1)}$ the local or one-step Lyapunov exponent. The long-time behavior of the orbit is determined by the asymptotic value of the Lyapunov exponent,

$$\lambda = lim_{k \to \infty} \frac{1}{k} ln |\alpha^{(k)}|. \tag{15}$$

Clearly, an accurate numerical determination of (15) is in many cases prohibitively complicated. The best one can hope for is that the exponents $\lambda^{(k)}$ for large $k(k \approx 10^5)$ are close to their asymptotic values.

According to (13b) the four-dimensional mapping A^k permits two positive Lyapunov exponents ($\lambda_i, i = 1, 2$). The extraction of all positive Lyapunov exponents is complicated by the fact that in high-dimensional systems usually the largest positive Lyapunov exponent λ_1 dominates the exponential separation of nearby orbits, since

$$lim_{k \to \infty} e^{\lambda_2 k} / e^{\lambda_1 k} \to 0. \tag{16}$$

We, therefore, restrict ourselves in the following to the largest exponent λ_1. Work is in progress to determine the complete set of exponents in the limit $k >> 1$.

We note parenthetically that the four-dimensional mapping allows for "Arnold diffusion"[11]. The KAM tori do not topologically separate different regions of chaotic

motion in phase space for time-dependent Hamiltonian systems with ≥ 2 degrees of free-dom (or time-independent systems with ≥ 3 degrees of freedom). Therefore, all stochastic islands are connected by the Arnold web leading to slow global stochastic diffusion. We are presently investigating Arnold diffusion for the periodically kicked hydrogen atom.

While the evolution of individual trajectories such as the one shown in Fig. 2 gives a qualitative insight into the dynamics, a comparison with the experiment or a quantum mechanical description requires the investigation of classical ensembles. Different ensembles should be distinguished:

a) the average over the angle variables τ and ψ which allows to approximately simulate a quantum state (n, ℓ, m) by a classical ensemble. Note that ψ corresponds to the Euler angle γ in Rose's notation[17],

b) the average over the remaining Euler angles which corresponds to a isotropic statistical mixture of all m substates,

c) the average over all ℓ states which corresponds to the microcanonical ensemble and

d) in the case of a noisy system an ensemble average over "heat bath" variables, i.e. fluctuating forces.

3. RESULTS

The local stability of the orbit (or an ensemble of orbits) can be measured by the one-step Lyapunov exponent $\lambda^{(1)}$. The dependence of the largest exponent $\lambda^{(1)}_1$ for an isotropic ensemble and k=400 is displayed in Fig. 3. The ensemble average extends over the phase angle τ and ψ and the Euler angles of $n = 100$ orbits with different fixed ℓ values. The ℓ values are chosen such that the squared eccentricity

$$\epsilon^2 = 1 - (\ell/n)^2 \tag{17}$$

takes the approximate values $\approx 1(\ell = 1), 0.5(\ell = 67.4)$ and $0(\ell = 99)$. For small kick amplitudes $\Delta \tilde{P} << 1$ the power law dependence of $\lambda^{(1)}_1$,

9

$$\lambda_1^{(1)}(\Delta \tilde{P}) = C\Delta \tilde{P}^\delta \tag{18}$$

shows a "critical" exponent close to $\delta = 1/2$ irrespective of ℓ. This value of δ can be easily understood by the following simple (non-rigorous) argument: For small perturbations the maximum Lyapunov exponent $\lambda_1^{(1)}$ can be assumed to be small, i.e. the corresponding (real) eigenvalue of the stability matrix is close to unity,

$$\alpha_1 \approx 1 + \Delta \alpha_1 \tag{18}$$

We can furthermore neglect the deviation of the second eigenvalue from unity ($\Delta \alpha_2 \approx 0$). The trace of the stability matrix, therefore, becomes

$$\begin{aligned} Tr\, A^{(1)} &= 2 + (1 + \Delta\alpha_1) + \frac{1}{1 + \Delta\alpha_1} \\ &\simeq 4 + \Delta\alpha_1^2 + O(\Delta\alpha_1^3) \end{aligned} \tag{19}$$

On the other hand, a power series expansion of the mapping (7) in ΔP leads to

$$Tr\, A^{(1)} = 4 + C^2 \Delta \tilde{P} + O(\Delta \tilde{P}^2) \tag{20}$$

where the expansion coefficient C^2 depends on $\tilde{\ell}, \tilde{\omega}$, the Euler and phase angles. Combining (19) and (20) gives

$$\Delta \alpha_1 = C\Delta \tilde{P}^{1/2} \tag{21}$$

and consequently,

$$\begin{aligned} \lambda_1^{(1)} &= \ell n(1 + \Delta\alpha_1) \\ &\simeq C\Delta\tilde{P}^{1/2}, \end{aligned} \tag{22}$$

in agreement with (18). The expansion (20) becomes invalid for larger $\Delta \tilde{P}$. We observe deviations from (22) for $\Delta \tilde{P} \gtrsim 0.1$. We have also found a strong dependence of C on ℓ:

Low ℓ states with ϵ^2 close to 1 show a significantly enhanced instability. The origin of the nonmonotonic ℓ dependence of $\lambda_1^{(1)}$ displayed in Fig.3 is not yet fully understood.

The strong local instability of low ℓ states has important consequences for the evolution of Rydberg atoms under the influence of multiple collisions. Primary production processes of Rydberg atoms such as laser and collisional excitation tend to prefer low ℓ states[18]. Their enhanced instability suggests that interactions with the environment will lead to rapid ℓ diffusion to higher ℓ states. Such a rapid ℓ redistribution has been recently observed in doubly excited $C^{2+}(2p5\ell)$ states produced in ion-solid collisions[19] and have been quantitatively explained in terms of stochastic ℓ diffusion[20].

Since the collisional perturbations which can be realistically modelled by δ-shaped pulses (e.g., transport of excited projectile states through solids) are stochastic, the observed ℓ diffusion may be due to either extrinsic or intrinsic stochasticity. In order to delineate the contributions to transport due to intrinsic instability and due to "noise" we have performed a comparative calculation of $\lambda_1^{(1)}$ for both periodic and stochastic perturbations under otherwise identical conditions. We have chosen a fixed scaled frequency $\tilde{\omega} = 3/2$ and introduced amplitude-modulated noise with a Gaussian distribution in ΔP_i with the variance $\text{Var}(\Delta P_i) = \Delta P^2$ identical to that of the periodic perturbation. For an isotropic ensemble of $\ell = 67.4$ states and 400 kicks (Fig. 4) we find that for small pulse heights $\Delta \tilde{P} < 10^{-2}(\Delta P < 10^{-4})$ the stochasticity is predominantly extrinsic Lyapunov exponent is almost one order of magnitude larger for stochastic perturbations than for periodic perturbations. For larger $\Delta \tilde{P} \gtrsim 10^{-2}(\Delta P \gtrsim 10^{-4})$ the relative weight shifts toward intrinsic stochasticity. The difference between the two λ values becomes small. In other words, the random amplitude modulation loses its importance compared to the effect of intrinsic stochasticity. The present calculation of λ_1 employing action-angle variables (Eq. 7) could not be extended beyond $\Delta \tilde{P} \gtrsim 0.1 (\Delta \tilde{P} \gtrsim 10^{-3})$ since for larger ΔP all orbits have ionized after 400 kicks.

The ionization probability for these ensembles as a function of ΔP are shown in Fig.5, together with the fraction of regular orbits (i.e. orbits with vanishing Lyapunov exponent). Because of numerical uncertainties we have set a threshold value of $\lambda_1 \gtrsim 10^{-5}$ for the Lyapunov exponent to be non-zero. For $\Delta P < 2 \times 10^{-4}$ all orbits remain bound after 400 kicks. In this domain the periodic perturbation allows a significant fraction ($\simeq 20\%$) of orbits (i.e. of the phase space) to be regular while the noise destroy almost all regular orbits even at small values $\Delta P \simeq 10^{-5} (\Delta \tilde{P} \simeq 10^{-3})$. Note that the increase of the average value of λ_1 seen in Fig. 4 is due to both to the increase of the fraction of chaotic orbits shown in Fig. 5 as well as to the increase of the numerical value of λ_1 for the chaotic orbits. For $\Delta P > 2 \times 10^{-4}$ we observe a rapid increase of the fraction of ionized orbits. Choosing the 50% level as a threshold, the kicked hydrogen atom in a $n = 100, \ell = 67.4$ state ionizes at a periodic amplitude $\Delta P = 6 \times 10^{-4}$ and at a Gaussian randomly distributed amplitude $\Delta P = 3 \times 10^{-4}$, i.e. the noisy perturbation reduced the ionization threshold by approximately a factor 2.

The observation of complete ionization of the impulsively driven Rydberg atom raises the question as to the underlying ionization mechanism. More specifically, is the ionization "chaotic" — is it the result of a "random walk" in bound Coulomb states space which finally reaches the continuum? For ionization by a monochromatic microwave field it is well-known that the ionization mechanism is partially chaotic[19,20]. A preliminary answer to this question for the impulsively driven hydrogen atom can be deduced from a study of the time reversal symmetry of the mapping (Eq. (7)) in a computer experiment. The equation of motion of a Hamiltonian system, and therefore the resulting mapping, satisfies time reversal symmetry, i.e.

$$T^{(-k)} \circ T^{(k)} = 1 \qquad (23)$$

where $T^{(-k)}$ denotes the evolution operator for k kicks backward in time. The ubiquitous numerical noise in a computer experiment will break the exact time reversal symmetry.

12

Random fluctuations accumulated during the forward evolution $T^{(k)}$ will not cancel out in the subsequent backward evolution. Consequently, the system will not exactly return to this initial condition. The deviation D,

$$D = |T^{(-k)} \circ T^{(k)}(X_0) - X_0| \tag{24}$$

where X_0 denotes the vector of phase space coordinates of the initial state, is a measure of the chaoticity of the orbit. If the orbit is regular and $\lambda_1 = 0$ numerical noise leads only to a slow growth of D which is related to the numerical precision within each iteraction. In our case, numerical errors result predominately from the solution of the transcendental equation [16] for the Kepler orbit with a typical accuracy of $\approx 10^{-10}$. On the other hand, for chaotic orbits errors will grow exponentially with the rate of the largest Lyapunov exponent, destroying any memory of the initial state and precluding the return to the initial state.

We have tested the extent of the breakdown of time reversal symmetry for a microcanonical ensemble of $n = 100$ Rydberg atoms driven by a periodic impulsive force with scaled frequency $\tilde{\omega} = 3/2$ and scaled amplitude $\Delta\tilde{P} = 0.1$ (Fig. 6). The fraction of orbits in continuum states, $W(E > 0)$, and those in states higher than $n = 150, W(n \geq 150)$, show only a weak breakdown of time reversal symmetry. While after the forward evolution of $k = 120(60$ periods) more than 50% are in very high Rydberg states and 7% are already ionized, all orbits are bound again and only 5% are still above $n = 150$ upon completion of the backward evolution. We note that our results for $W(n \geq 150)$ resemble those of Ref. 10. The complete reversibility of the ionization curve, $W(E > 0)$, strongly indicates that the underlying ionization mechanism is regular and non-chaotic. The physical interpretation is as follows: For kicks with amplitude comparable to the internal orbital momentum a few kicks are sufficient to reach the continuum, in particular, if one on several of them occur near the nucleus where the energy transfer is maximal[21]. This situation is similar to that of multi-photon ionization where a relatively small number of absorption

13

processes suffice to reach above threshold states. Ionization is in this case not the termination point of a "random walk" in the space of bound states but rather the result of a short, directed few-step excitation process. Therefore, ionization of the impulsively driven hydrogen cannot be taken as an indicator of chaotic dynamics. This is in sharp contrast to the ionization by monochromatic microwave where the chaotic pathway to ionization has been clearly established[19,20]. The marked difference is an obvious consequence of the difference between Fourier spectrum of the perturbation (Eq. (8)) and a monochromatic perturbation. The high-frequency components of the δ-shaped pulse allow direct transitions to the continuum and therefore overshadow the stochastic pathway to ionization.

4. CONCLUSIONS

The motion of the classical three-dimensional hydrogen atom driven by a sequence of pulses is chaotic. The observed stochasticity is due to both intrinsic stochasticity of the deterministic system with strictly periodic pulses and due to extrinsic stochasticity of a noisy spectrum of random pulses. The relative importance of the two mechanisms for chaotic motion, as measured by the Lyapunov exponent, changes as a function of the amplitude of the kicks. For very small amplitudes stochastic dynamics is predominantly extrinsic while for larger amplitudes ($\Delta\tilde{P} \gtrsim 10^{-2}$) the Lyapunov exponent for the periodically and randomly driven system become comparable. For amplitudes $\Delta\tilde{P} \gtrsim 0.1$ where the momentum transferred in a single kick becomes comparable to the orbital momentum rapid excitation to very high-lying bound states and continuum states takes place, thereby suppressing stochastic motion. These findings suggest the existence of a chaotic n "window" for the periodically kicked hydrogen atom with fixed amplitude ΔP: For low n the scaled amplitude $\Delta\tilde{P}$ is sufficiently small such that the motion remains predominantly regular. For higher n the scaled amplitude $\Delta\tilde{P}$ is so large that rapid transitions to near-threshold states lead to regular motion. In between a window of chaotic n states exists where $\Delta\tilde{P}$ is,

large enough to result in a strong perturbation but also small enough to prevent rapid ionization. In this regime the electronic motion resembles that of a random walk in Coulomb state space.

Further work is needed along different lines: In the present numerical investigations, we have restricted ourselves to a few hundred iterations of the mapping. In order to determine the long-term stability of classical orbits it is necessary to extend the calculation to much larger numbers of kicks. Futhermore, the modification of the dynamics of chaotic systems due to quantum effects are presently under intensive investigation[3,6,7,22]. For the kicked hydrogen atom a detailed analysis of quantum dynamics of a classically chaotic three-dimensional system should become possible.

DISCLAIMER

References

1. M. Henon and C. Heiles, Astron. J. 69, 73 (1964).

2. B. Chirikov, F. Izrailev, D. Shepelyansky, Sov. Sci. Rev. C2, 709 (1981).

3. P. Koch, in <u>Electronic and Atomic Collisions</u>, eds. H. Gilbody, W. Newell, F. Read and A. Smith, Elsevier Science Publ., Amsterdam, (1988) p.501.

4. For an overview see A. Lichtenberg and M. Liebermann, <u>Regular and Stochastic Motion</u>, (Springer-Verlag, NY, 1983).

5. V. Arnold, and A. Avez, Ergodic Problems of Classical Mechanics (Benjamin, NY, 1968).

6. D. Delande and J.C. Gay, Comments. At. Mol. Phy. 19, 35 (1986) and ref. therein.

7. A. Dhar, M. Nagaranjan, F. Izrailev, R. Whitehead, J. Phys. B16, L17 (1983). A. Carnegie, J. Phys. B17, 3435 (1984).

8. R. Blümel and U. Smilansky, Phys. Rev. A30, 1040 (1984).

9. J. Leopold, D. Richards, J. Phys. B21, 25 (1988); J. Leopold and D. Richards, J. Phys. B19, 1125 (1986).

10. T. Grozdanov and H.S. Taylor, J. Phys. B20, 3683 (1987).

11. V. Arnold, Sov. Math. Dokl. 5, 581 (1964).

12. Y. Yamazaki et. al., Phys. Rev. Lett. 61, 2913 (1988)

13. J. Burgdörfer and C. Bottcher, Phys. Rev. Lett. 61, 2917 (1988).

14. F.B. Dunning and R.F. Stebbings, "Rydberg States of Atoms", Comments Atom. Mol. Phys. 10, 9 (1980). H.J. Metcalf, Nature **284**, 127 (1980). C. Burkhardt, R. Corey, W. Garver, J. Leventhal, M. Allergrini, L. Loi, Phys.

Rev. A34, 80 (1986). G. Vitrant, J.M. Raimond, M. Gross and S. Haroche, J. Phys. B15, L49 (1982).

15. I. Percival and D. Richards, J. Phys. B12, 7051 (1979).

16. L. Landau and E. Lifshitz, A course in theoretical physics, Vol. 1 (Pergamon Press, Oxford, 1973).

17. M. Rose, Elementary Theory of Angular Momentum, (Wiley, NY, 1957); see also M. Born, Vorlesungen über Atommechanik, (Springer, Berlin, 1925, (reprint 1976)).

18. We note that the recently observed selective laser excitation of "circular" Rydberg states can reach higher ℓ values, see R. Hulet and D. Kleppner, Phys. Rev. Lett. 51, 1430 (1983).

19. R. Jensen, Phys. Rev. A30, 386 (1984).

20. R. Jensen, J. Leopold, and D. Richards, J. Phys. B21, L527 (1988).

21. J. Burgdörfer in "Lecture Notes in Physics", Vol. 294, (eds. D. Berényi and G. Hock, Springer-Verlag, Berlin, 1988) p. 344.

22. For a review see, B. Eckart, Phys. Rep. 163, 205 (1988).

Fig. 1

Random walk in the $\epsilon - \ell$ plane of the phase space for an impulsively driven Rydberg atom.

Fig. 2

Projection of the phase space evolution according to Eq. (7) projected onto the (n, τ) and (ℓ, ψ) planes (see text). a) $\Delta P = 10^{-4}$;   b)$\Delta P = 3.5 \times 10^{-4}$
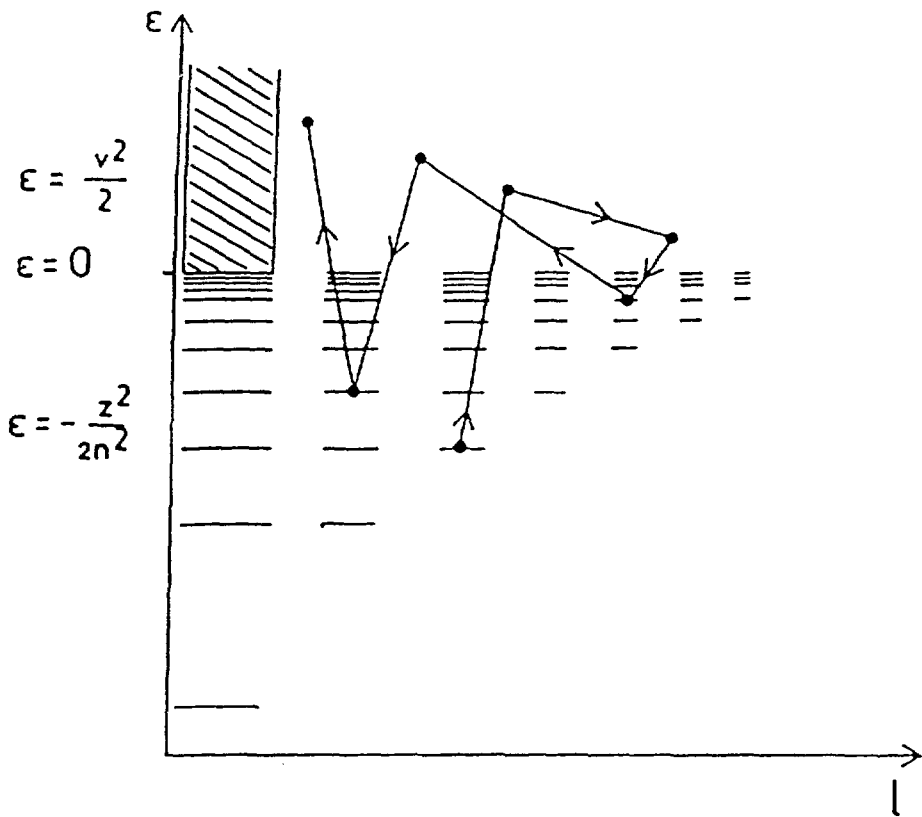
Fig. 3

Local one-step Lyapunov exponent $\lambda_1^{(1)}$ averaged over an isotropic ensemble of $n = 100$ orbits as a function of ΔP. $\circ : \ell = 1$; $\bullet : \ell = 67.4$; $\triangle : \ell = 99$.

Fig. 4

Lyapunov exponent $\lambda_1^{(400)}$ averaged over an isotropic ensemble of $n = 100$, $\ell = 67.4$ orbits as a function of ΔP. $\bullet$: periodic pulses $\blacktriangle$: Gaussian amplitude-modulated noise.
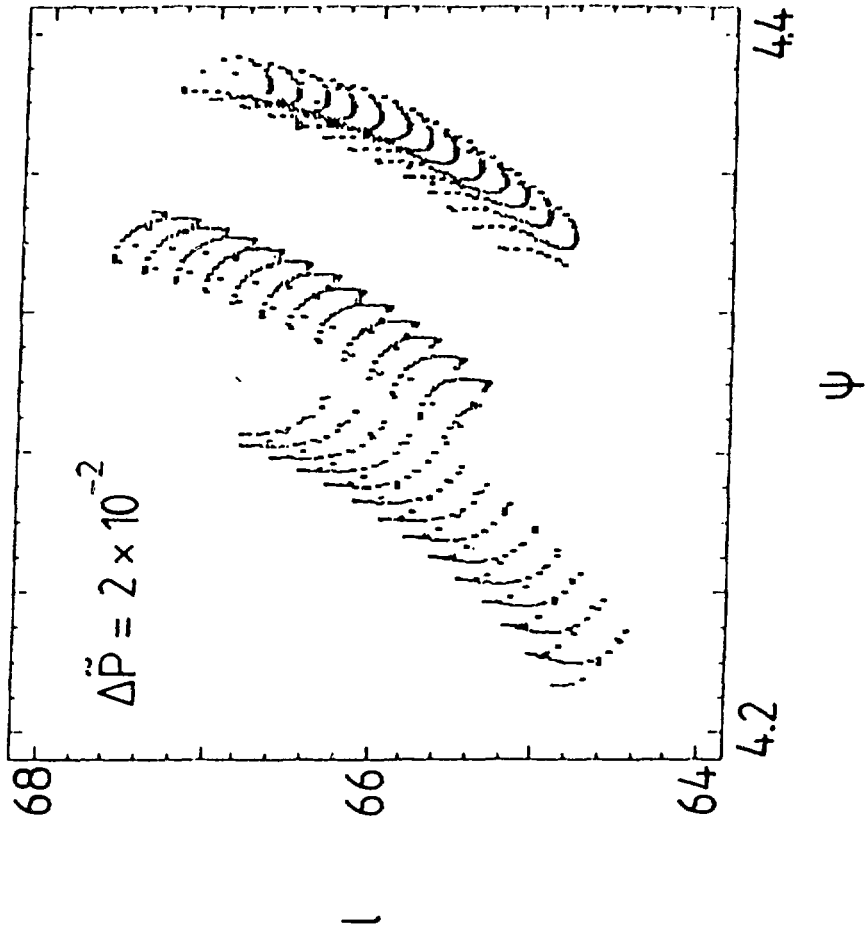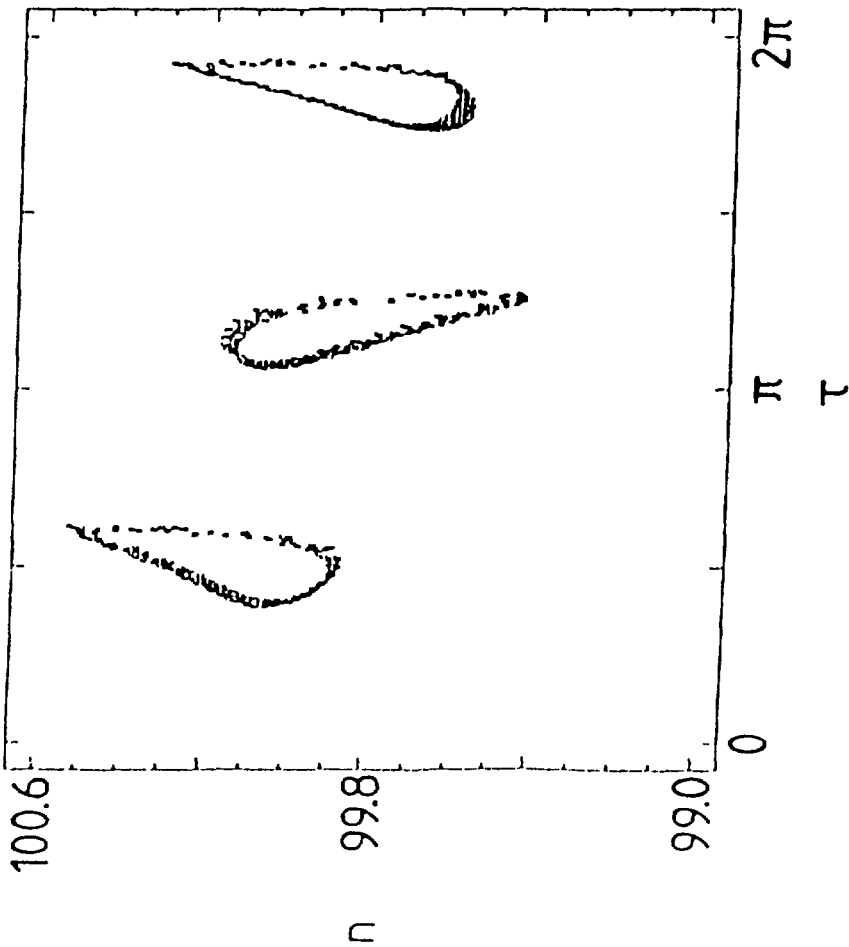
Fig. 5

Fractions of regular $(\bullet, \blacktriangle)$ and ionized $(\circ, \triangle)$ $n = 100$ $\ell = 67.4$ orbits after 400 pulses. $(\bullet, \circ)$: periodic pulses;$(\blacktriangle, \triangle)$: Gaussian amplitude-modulated noise.
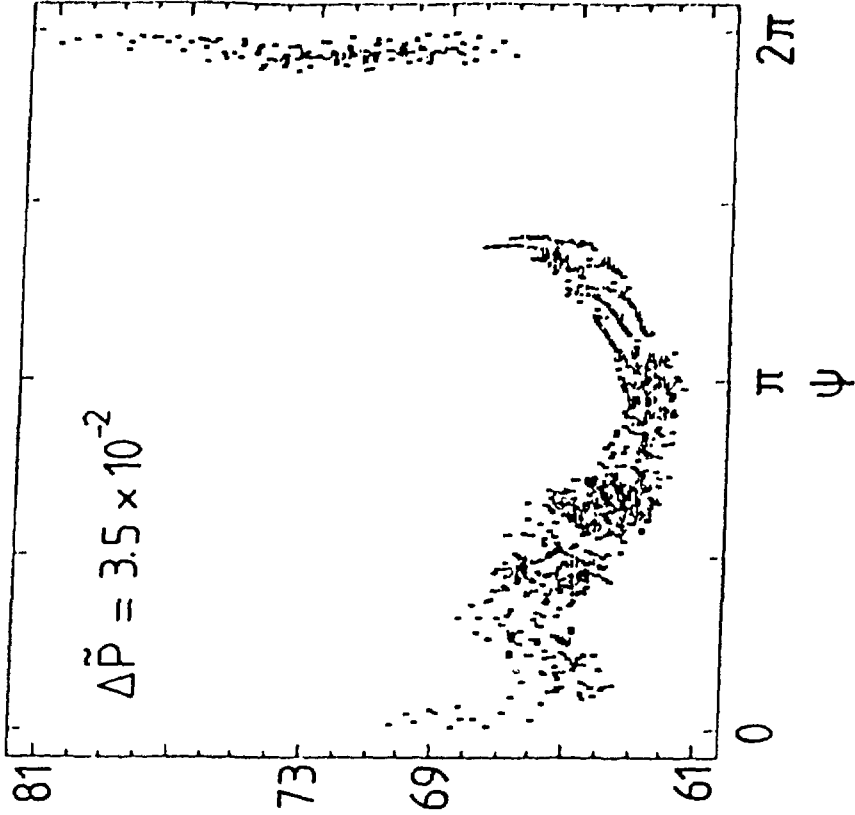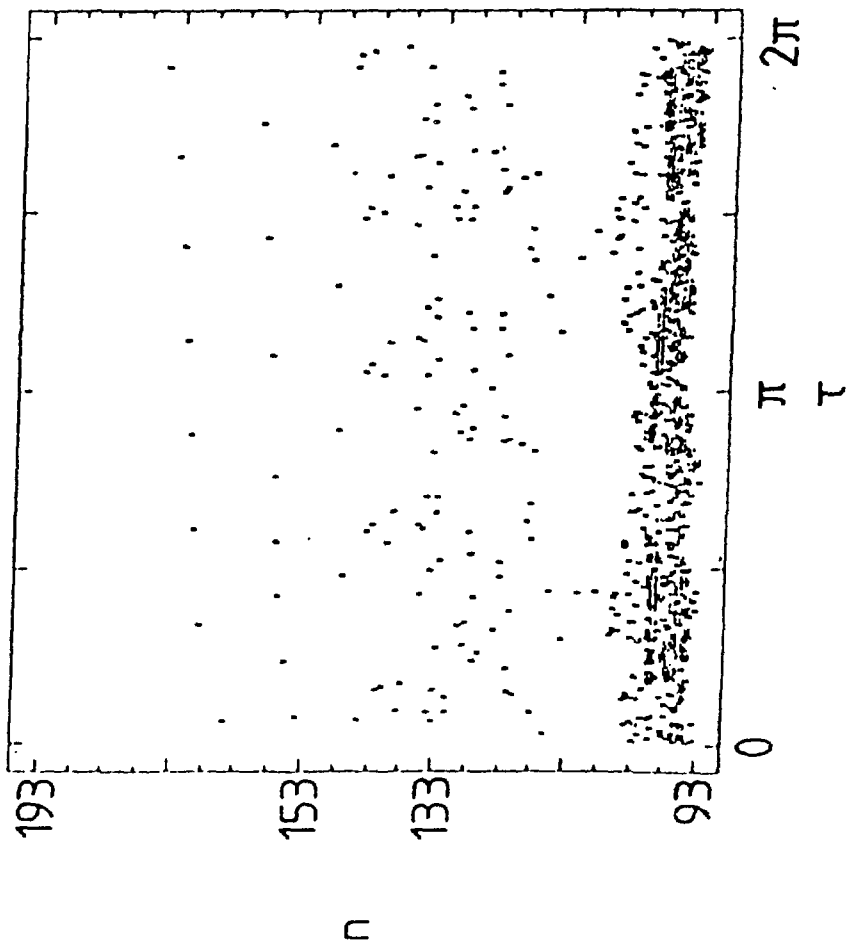
Fig. 6

Fraction of highly excited, $W(n \geq 150)$ and ionized orbits, $W(\quad)$ for the periodically kicked Rydberg atom. Initial conditions: $n = 100$ microcanonical ensemble, $\tilde{\omega} = 3/2$, and $\Delta P = 1.06 \times 10^{-3}$. The ensemble is propagated backward in time after 60 periods $(k = 120)$.
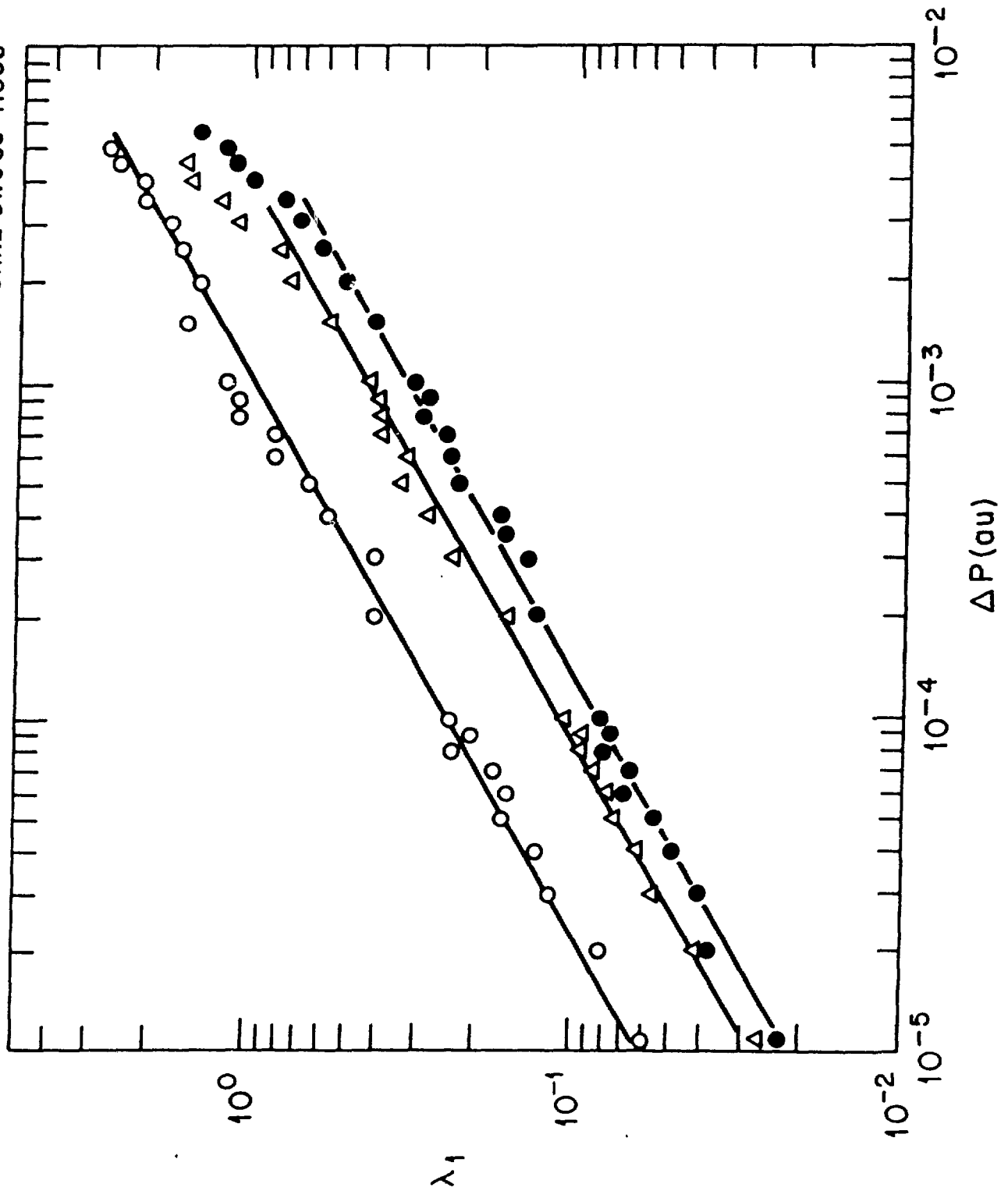
1

$$\epsilon = \frac{v^2}{2}$$

$$\epsilon = 0$$

$$\epsilon = -\frac{z^2}{2n^2}$$

(a)

$\Delta \tilde{P} = 2 \times 10^{-2}$

100.6

99.8

99.0

0   π   2π

τ

U

68

66

64

4.2   4.4

ψ

I

(b)

$\Delta\tilde{P} = 3.5 \times 10^{-2}$

ORNL-DWG 88-11068

ORNL-DWG 88-11067

ORNL–DWG 88–11062